

MiR-429 regulates the proliferation and apoptosis of nephroblastoma cells through targeting c-myc

H.-F. WANG¹, W.-H. WANG¹, H.-W. ZHUANG¹, M. XU¹

¹Department of Pediatric Surgery, Linyi Central Hospital, Linyi, China

Haifeng Wang and Wenhua Wang contributed equally to this work

Abstract. – OBJECTIVE: We explored the regulation of miR-429 in nephroblastoma cells, investigating the mechanisms by which miR-429 influenced the proliferation and apoptosis of nephroblastoma.

PATIENTS AND METHODS: The quantitative reverse transcription polymerase chain reaction (qRT-PCR) was conducted to detect the expression of miR-429 in nephroblastoma tissues and cell lines (G401). The interaction between miR-429 and c-myc was confirmed by qRT-PCR, Western blotting and luciferase assays, respectively. MTT (3-(4,5-dimethylthiazol-2-yl)-2,5-diphenyl tetrazolium bromide) and clone formation assay were used to detect the effect of miR-429 on the proliferation and clone formation ability of G401 cells. Cell cycle and apoptosis of G401 cells were measured by flow cytometry and TUNEL staining, respectively.

RESULTS: miR-429 was down-regulated in nephroblastoma tissues and cells. On-line target gene prediction software was applied to screen c-myc, the potential downstream target gene of miR-429. The expression of c-myc was negatively regulated by miR-429. Subsequent experiments demonstrated that overexpression of miR-429 inhibited the proliferation ability and arrested cell cycle of G401 cells in G0/G1 phase. Besides, the number of apoptotic cells was increased in miR-429 intervened group. However, c-myc could reverse the biological effects of miR-429 on proliferation, apoptosis, clone formation and cell cycle of G401 cells.

CONCLUSIONS: MiR-429 can regulate the proliferation, clone formation, cell cycle and apoptosis of nephroblastoma cells through targeting c-myc, indicating miR-429 may function as a potential therapeutic target for the treatment of nephroblastoma.

Key Words:

MiR-429, Nephroblastoma, C-Myc, G401.

Introduction

Nephroblastoma is the most common primary malignant tumor of the urinary system in children. In 1899, Doctor Max Wilms in Germany described nephroblastoma in detail for the first time, so it is also known as Wilms' tumor (WT)¹. Nephroblastoma often occurs in children younger than 5 years old, the incidence rate of which accounts for about 8-10% in children's malignant tumors and 95% in children's renal tumors^{2,3}. The pathogenesis of nephroblastoma in children is complex. Currently, researches have revealed that the abnormal activation of oncogenes, lack or inactivation of tumor suppressor genes, point mutations of relevant genes or abnormal gene regulation in child patients, are related to the occurrence of nephroblastoma⁴. The comprehensive treatments, including surgery, chemotherapy and radiotherapy, significantly improve the prognosis of child patients with nephroblastoma. However, traditional treatment has unsatisfactory curative effects on nephroblastoma patients with poor histological features and relapse after treatment^{5,6}. Therefore, in-depth investigations on the biological characteristics and pathogenesis of nephroblastoma were of great clinical value and significance in searching new treatment methods and improving the survival rate of child patients.

In recent years, the correlation between micro ribonucleic acid (miRNA) and tumors has been attracted increased attention. MiRNA is a kind of non-coding small RNA with 18-25 nt in length, which regulates the post-transcriptional translation of the target gene mRNA through binding to its 3'-untranslated region (3'-UTR)⁷. It had been proved that miRNA played an important role in

the regulation of gene expression and biological growth and development, including cell cycle, cell growth, apoptosis, embryonic development, stress response, metabolism, morphogenesis and formation of various diseases^{8,9}. According to statistics¹⁰, miRNA found in the human genome might regulate one third of human genes. Similar to other tumors, a large number of differentially expressed miRNAs have been found in nephroblastoma. Several works have already confirmed the potential clinical application of these certain miRNAs in nephroblastoma. For example, miR-1180-5p¹¹ and miR-21¹² acted as oncogenes, which promoted the malignant behavior of nephroblastoma by targeting the expressions of p73 and PTEN, respectively. However, the low expression of miR-613 in nephroblastoma had a tumor-suppressive effect on nephroblastoma's progression and metastasis *via* mediating the expression of FRS2¹³.

As a member of miRNAs, miR-429 had been found involving in the occurrence and development of many kinds of tumors¹⁴⁻¹⁷. However, there were few studies on the roles of miR-429 in the development of nephroblastoma.

In this study, it was found that the expression level of miR-429 in nephroblastoma tissues was significantly decreased, and the biological role of miR-429 in nephroblastoma cells was further studied.

Patients and Methods

Patients

37 pairs of nephroblastoma tissues and adjacent normal tissues were obtained from nephroblastoma patients undergoing surgical procedure at Linyi Central Hospital. Patients were pathologically confirmed as nephroblastoma. Tissues were frozen in the liquid nitrogen and kept at -80°C refrigerator. Both adjacent normal tissues and nephroblastoma tissues should be confirmed by biopsy detection. This study was approved by the Ethics Committee of Linyi Central Hospital. Signed written informed consents were obtained from all parents or guardians of the patients before the study.

The human nephroblastoma cell line (G401) together with human embryonic kidney cell line (HEK-293T) were purchased from the Chinese Academy of Sciences (Shanghai, China). All cells were cultured in Roswell Park Memorial Institute 1640 (RPMI-1640) medium (Gibco, Rockville, MD, USA) complemented with 10% fetal bovine serum (FBS), 100 µg/mL streptomycin and 100

IU/mL penicillin (Gibco, Rockville, MD, USA) in 5% CO₂ cell culture incubator.

Luciferase Reporter Assays

In TargetScan, miRDB and microRNA websites, it was found that c-myc was a target gene of miR-429. The binding sequence of miR-429 at the 3'-end of c-myc was mutated using a point mutation kit (Agilent Technologies, Santa Clara, CA, USA). The mutated c-myc (Mut-type) and non-mutant c-myc (WT-type) were connected with the pGL3-Basic luciferase reporter vector (Promega, Madison, WI, USA). PGL3-basic vector with mutant c-myc was transfected into G401 cells after lentivirus intervention in the 24-well plate. The same treatment was performed on the pGL3-basic vector connected with the non-mutant c-myc according to steps in the Luciferase Reporter Gene Assay Kit. The luciferase activity was detected in a multi-function microplate reader.

Transfection

MiR-429 mimics and si-c-myc were synthesized and transfected to nephroblastoma cell lines (G401) to analyze biological function of miR-429. Three groups were established to study the potential relevance between miR-429 and G401 cell, namely NC group (negative control), miR-429 mimics (G401 cells transfected with miR-429 mimics) and mimics + c-myc (G401 cells transfected with miR-429 mimics and si-c-myc). All plasmids were purchased from RiboBio (Guangzhou, China), and transfected using lipofectamine RNAiMAX (Life Technologies, Gaithersburg, MD, USA) according to the manufacturer's instructions.

Quantitative Reverse Transcription Polymerase Chain Reaction (qRT-PCR) Analysis

Total RNA was procured by TRIzol Reagent (Invitrogen, Carlsbad, CA, USA) in accordance with the manufacturer's protocol. SYBR green qPCR assay was used to measure the expression level of c-myc and endogenous controlled by glyceraldehyde 3-phosphate dehydrogenase (GAPDH). TaqMan miRNA assay (Applied Biosystems, Foster City, CA, USA) was used to measure the level of miR-429 expression normalized to miRNA U6. Primer sequences used in this study were as follows: c-myc, F: 5'-TCGGACTCTCTGCTCTCCTC-3', R: 5'-CTG-CATAATTGTGCTGGTGC-3'; microRNA-429, F: 5'-GCCGATTAATACTGTCTGGTAA-3', R: 5'-CAGTGCAGGGTCCGAGGT-3'; U6: For-

ward: 5'-CTCGCTTCGGCAGCACA-3', Reverse: 5'-AACGCTTCACGAATTTGCGT-3'

Western Blot Analysis

The protein concentration was measured by bicinchoninic acid (BCA) reagent kit (Merck, Billerica, MA, USA). 20 µg protein of G401 cells was subjected to 10% sodium dodecyl sulfate (SDS) polyacrylamide gel electrophoresis, transferred onto a nitrocellulose membrane and sealed with gelatin for 2 h. Membranes were incubated with anti-c-myc and anti-GADPH (diluted at 1:1000, Cell Signaling Technology, Danvers, MA, USA) at 4°C overnight. Subsequently, membranes were incubated with specific horseradish peroxidase-conjugated secondary antibody (1:10000) for 1 h, and washed with Tris-Buffered Saline with Tween-20 (TBS-T) for 3 times. The protein bands were developed using enhanced chemiluminescence (ECL) method (Thermo Fisher Scientific, Waltham, MA, USA). The proteins were visualized and detected, and the grey level of each protein was normalized to the GADPH. Western blot results were analyzed *via* Image-J software.

Cell Proliferation

Cells in logarithmic growth phase were collected, diluted into 1×10^6 cell suspension, and added into a 96-well cell culture plate ($5 \times 10^3/100$ µL per well). Blank controls were set with only culture medium. Cell viability was determined *via* MTT (3-(4,5-dimethylthiazol-2-yl)-2,5-diphenyl tetrazolium bromide) assay. 15 µL MTT reagent (500 µg/mL) were added to each well. Cells were continuously cultured at 37°C for 2 h, followed by the measurement of the absorbance value at the wavelength of 450 nm. The blank control was zeroed, and absorbance value at the wavelength of 450 nm was measured using a microplate reader.

Clone Formation Assays

The G401 cells were digested and transfected with trypsin for in single cell suspension state. 6×10^3 cells were cultured in a 60 mm culture dish for 14 d, and bacterial colonies were fixed, stained with 0.5% crystal violet for 15 min. 10 random fields of view were observed under a light microscope, and the number of colonies was counted (cell groups consisting of more than 50 cells were taken as one cell colony).

Cell Cycle Assay

G401 cells were obtained 48 h after transfection, and 1×10^6 cells were collected from each

group. The cells were washed twice with phosphate-buffered saline (PBS), and the supernatant was discarded. During the cell cycle detection, each sample was added and fixed with 70% ethanol (pre-cooled at -20°C), placed at -20°C overnight. Subsequently, cells were washed twice with pre-cooled PBS, followed by 15 min of incubation with ribonucleases (RNases) (50 µg/mL) (Shanghai Li Rui Biological Technology Co, Ltd. Shanghai, China). After that, each sample was added with 50 µg/mL propidium iodide (PI) for 30 min of incubation. The stained cells were detected *via* flow cytometry. The rate of cells in G0/G1 or S phases was presented in the results.

Cell Apoptosis Detection

The apoptosis of G401 cells was detected by TUNEL assay according to the manufacturer's instructions (Roche, Basel, Switzerland). Horseradish peroxidase (HRP)-mediated diaminobenzidine reaction was used to visualize the TUNEL-positive cells, following the counterstain. Fields were photographed at a magnification of 200× and were randomly selected. The apoptosis index was used to measure the degree of apoptosis.

Statistical Analysis

Statistical Product and Service Solutions (SPSS) 16.0 software (SPSS Inc., Chicago, IL, USA) were used for statistical analysis. *t*-test was used for the intergroup differences. $p < 0.05$ was considered statistically significant.

Results

MiR-429 Expression was Reduced in Nephroblastoma Tissues and Cells

In order to examine the effect of miR-429 during the development of nephroblastoma, we measured the expression level of miR-429 in clinical tissues and adjacent normal tissues by qRT-PCR. The expression of miR-429 was remarkably lower in nephroblastoma tissues comparing with that in adjacent normal tissues (Figure 1). The same results were obtained in cellular level of miR-429 (Figure 2A). Taken together, we thought miR-429 might have regulatory effect during the progression of nephroblastoma.

C-myc is a Direct Target of miR-429

The microRNA target gene prediction software manifested that miR-429 could act on the 3'-UTR of c-myc. Firstly, we detected the ex-

pression level of c-myc in nephroblastoma cell lines by qRT-PCR, and we found that c-myc expression was up-regulated in G401 cells comparing with the control (Figure 2B-C). Secondly, luciferase activity was detected after co-transfection of constructed fluorescent report vectors (pmirGLO/c-myc-3'-UTR or pmirGLO/c-myc-3'-UTR mut) with miR-429 mimics into G401 cells, respectively. The results revealed that the over-expression of miR-429 could down-regulate the luciferase activity of the report vector of /c-myc-3'-UTR wt. However, the luciferase activity of c-myc-3'-UTR wt was up-regulated after the inhibition of miR-429 expression, suggesting that miR-429 had a targeting effect on c-myc. However, the luciferase activity in the report vector group transfected with mutant c-myc 3'-UTR did not decrease significantly (Figure 2D). Together, we thought that miR-429 and c-myc might have some correlation on effect during the progression of nephroblastoma.

MiR-429 Decreased the Expression Level of c-myc

The miR-NC group, miR-429 mimics group and the mimics + si-c-myc group were established to detect expressions of miR-429 and c-myc in G401 cells. The results from qRT-PCR and Western blotting showed that the expression level of c-myc was decreased by up-regulation of miR-429 in G401 cells. These data further illustrated the regulatory effect of miR-429 on the expression of c-myc (Figure 2E-G).

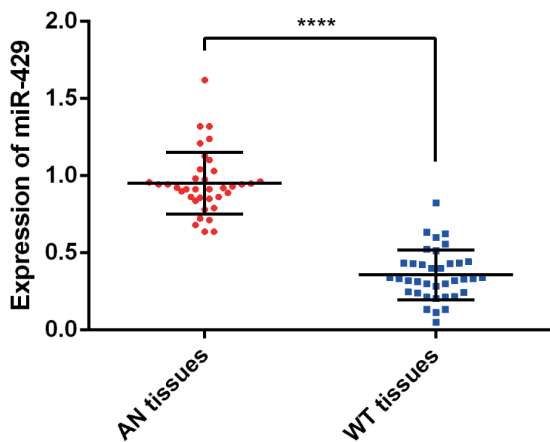


Figure 1. The expressions of miR-429 in nephroblastoma tissues. Difference in the expression of miR-429 between nephroblastoma tissues and adjacent normal tissues. (*****p*<0.0001).

MiR-429 Inhibited the Cell Proliferation

MTT assay was taken to detect the cell proliferation after the transfection. The results suggested that the cell proliferation of G401 cells were reduced by miR-429 mimics transfection. In contrast, the cell growth of nephroblastoma cells was found encouraged in mimics+ c-myc group (Figure 3A), indicating that miR-429 could inhibit the proliferation of nephroblastoma cells. Moreover, the colony formation in G401 cells transfected with miR-429 mimics was significantly decreased in number and size than those of control cells (Figure 3B).

The Influence of miR-429 on the Cell Cycle Proliferation

To explore whether miR-429 had an influence on cell cycle progression, it was observed that overexpression of miR-429 increased the percentage of cells in G0/G1 phase compared with that of S phase. However, an opposite effect was found after c-myc intervention. As a result, the study suggested that miR-429 could arrest cells in G0/G1 phase and promote cells in S phases for division and proliferation (Figure 3C, 3D).

MiR-429 Promoted the Cell Apoptosis

The apoptosis rate of G401 cells was detected by TUNEL assay. After the transfection of miR-429 mimics, the percentage of apoptotic cells was significantly increased (Figure 4A-B). However, the apoptotic rates were much lower in miR-NC and mimics+c-myc groups (Figure 4C). The results indicated the promotion effect of miR-429 on apoptosis of nephroblastoma cells.

Discussion

With the in-depth researches on miRNAs, there had been increasing studies focusing on the relationship between miRNA and tumors. The role of miR-429 in tumors has been well recognized. Researches had confirmed that the miR-429 expression in gastric cancer¹⁸ and colon cancer¹⁹ was significantly inhibited. MiR-429 was considered as a tumor suppressor miRNA in the pathogenesis of the above cancers. Overexpression of miR-429 could reduce the proliferation, migration and invasion capacity of tumor cells. The carcinogenesis of miR-429 was realized *via* regulating the FSCN1 and PAK6 expression. However, Huang et al²⁰ had demonstrated that upregulated miR-429 in liver cancer could promote the tumor cell proliferation,

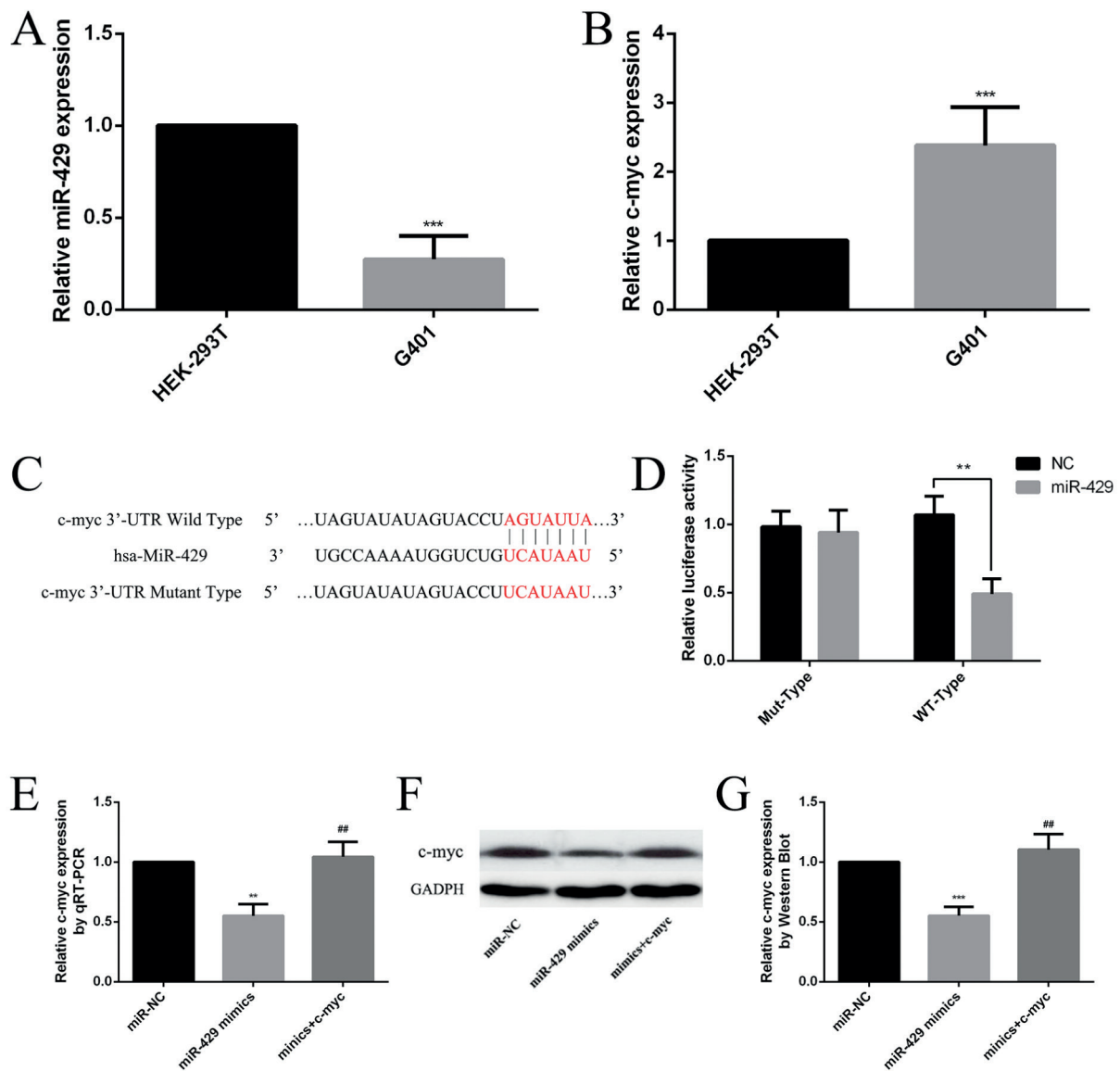


Figure 2. C-myc is a direct and functional target of miR-429. **A**, and **B**, Difference in the expressions of miR-429 and c-myc between human nephroblastoma cell line G401 and human embryonic kidney cell line HEK-293T (***) $p < 0.001$ vs. HEK-293T). **C**, Diagram of putative miR-429 binding sites of c-myc. **D**, Relative activities of luciferase reporters (**) $p < 0.01$). **E**, Expression level of c-myc by qRT-PCR analysis. **F**, Protein expression of c-myc by Western blot. **G**, Expression level of c-myc by Western blot experiment statistical analysis of **F**. All data were presented as means \pm standard deviations (**) $p < 0.01$, (***) $p < 0.001$ vs. NC group; (#) $p < 0.01$ vs. Mimics group).

indicating that miR-429 played a carcinogenic role in the development of liver cancer. To our best knowledge, there was no research on the biological function of miR-429 in nephroblastoma.

As previously mentioned, miRNA regulated the biological behavior of tumor cells by targeting the downstream genes, including the promotion of pro-

liferation, growth and invasion of tumor cells. To clarify the mechanism of miR-429 in affecting the occurrence and development of nephroblastoma, potential target genes of miR-429 were screened using on-line target gene prediction software. According to bioinformatics analysis, it was predicted that c-myc is a direct target gene of miR-429.

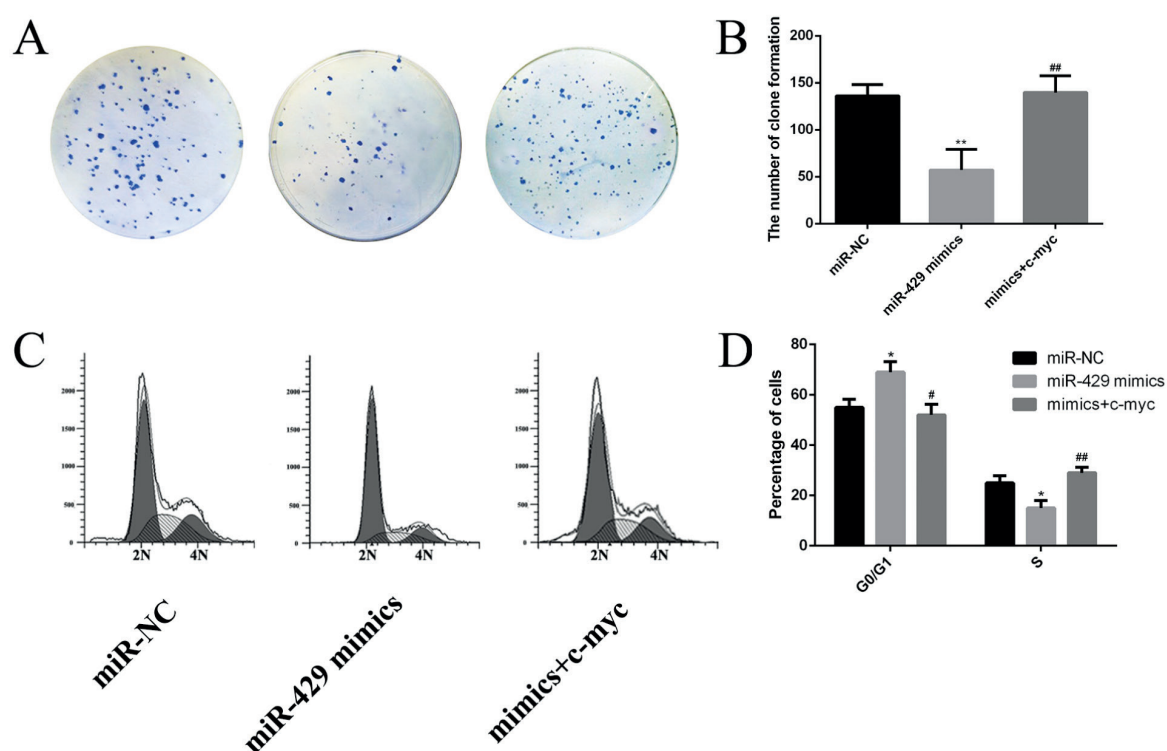


Figure 3. The influence of miR-429 on cell clone ability and cell cycle. **A**, Assessment of colony formation. **C**, The cell cycle phases of nephroblastoma cell analyzed using flow cytometry. **B**, and **D**, were statistical analysis of **A** and **B**, respectively. All data were presented as means \pm standard deviations (* p <0.05, ** p <0.01 vs. NC group; # p <0.05, ## p <0.01 vs. Mimics group).

C-myc, as a member of the proto-oncogene myc family, is located on chromosome 8, which mainly stimulates the cell proliferation and induces the apoptosis. Animal experiments had confirmed that overexpression of c-myc could promote cell deviation and induce quiescent cells into the cell division phase, thereby leading to increased cell proliferation rate and tumorigenesis. At the same time, c-myc expression was closely related to the proliferation and differentiation of such malignant tumors as non-small-cell lung cancer (NSCLC)²¹ and pancreatic cancer²². The regulatory effects of its expression in the aspect of cell growth, differentiation and malignant transformation had also been confirmed.

The microRNA target gene prediction software manifested that c-myc was a downstream target gene of miR-429. To further investigate the correlation between c-myc and miRNA in the occurrence and development of nephroblastoma, miR-429 mimics with or without si-c-myc were transfected into G401 cells. Western blotting and qRT-PCR results confirmed that there was a negative correlation between miR-429 and c-myc

expression in G401 cells. These results further proved that c-myc was a target gene of miR-143. Overexpression of miR-429 could significantly inhibit the proliferation and clone ability, whereas promote apoptosis of G401 cells. Furthermore, overexpression of c-myc could effectively reverse the effects of miR-429 on nephroblastoma cells. These results suggested that the inhibitory effect of miR-429 on the biological function of nephroblastoma cell was realized *via* inhibiting the expression of c-myc.

Conclusions

We showed the regulatory effect of miR-429 on the occurrence and development of nephroblastoma for the first time. The mechanism of miR-429 was further clarified to provide a new target for the biotherapy of nephroblastoma.

Conflict of Interest

The Authors declare that they have no conflict of interest.

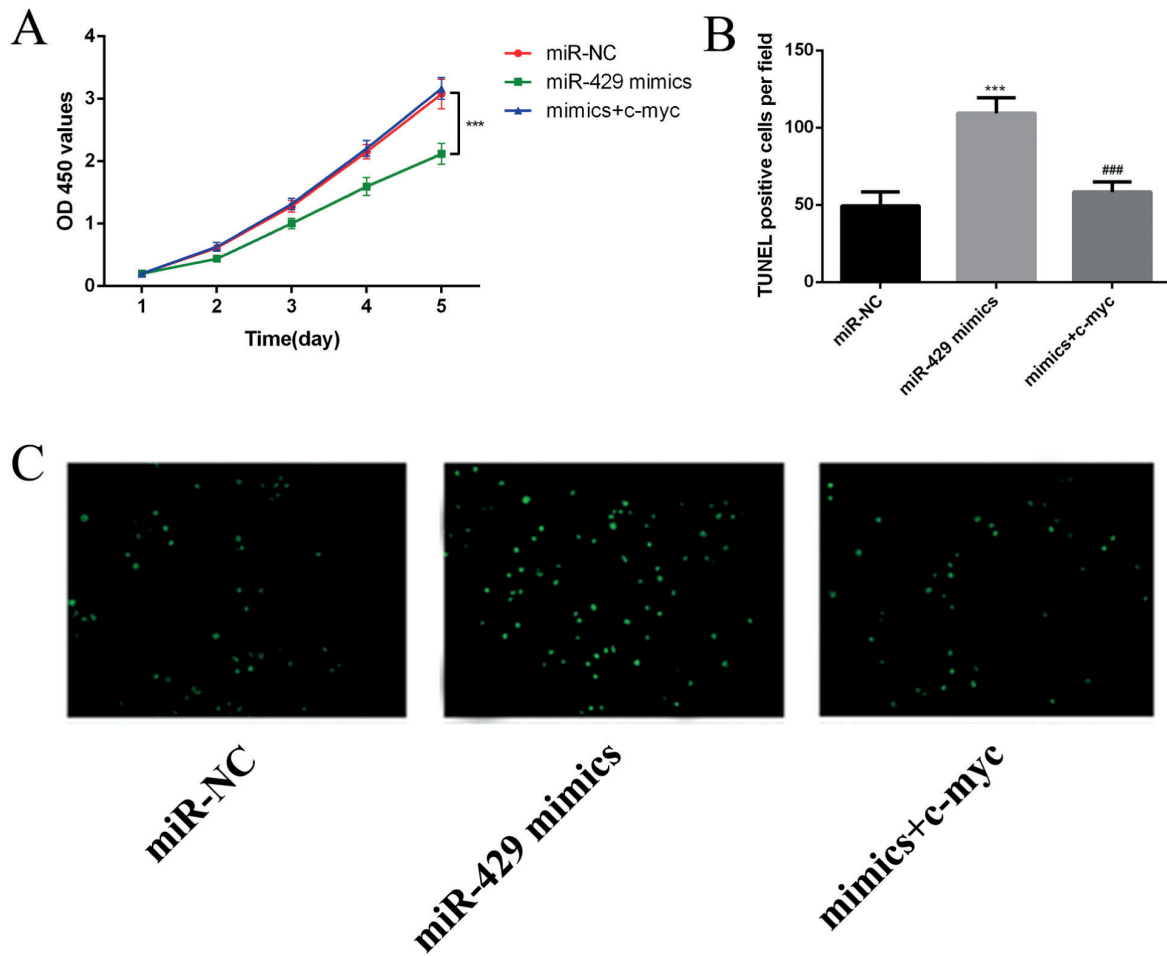


Figure 4. The influence of miR-429 on cell proliferation and cell apoptosis. **A**, Cell proliferation of nephroblastoma cells detecting by MTT assay ($***p < 0.001$). **B**, and **C**, Apoptosis level of ALL cells tested by TUNEL staining (200 \times). All data were presented as means \pm standard deviations ($***p < 0.001$ vs. NC group; $###p < 0.001$ vs. Mimics group).

Reference

- 1) RAFFENSPERGER J. Max Wilms and his tumor. *J Pediatr Surg* 2015; 50: 356-359.
- 2) CHAN CC, TO KF, YUEN HL, SHING CA, LING SC, LI CH, CHEUK DK, LI CK, SHING MM. A 20-year prospective study of Wilms tumor and other kidney tumors: a report from Hong Kong pediatric hematology and oncology study group. *J Pediatr Hematol Oncol* 2014; 36: 445-450.
- 3) DENG C, DAI R, LI X, LIU F. Genetic variation frequencies in Wilms' tumor: a meta-analysis and systematic review. *Cancer Sci* 2016; 107: 690-699.
- 4) KREPISCHI A, MASCHIETTO M, FERREIRA EN, SILVA AG, COSTA SS, DA CI, BARROS B, GRUNDY PE, ROSENBERG C, CARRARO DM. Genomic imbalances pinpoint potential oncogenes and tumor suppressors in Wilms tumors. *Mol Cytogenet* 2016; 9: 20.
- 5) GREEN DM. The evolution of treatment for Wilms tumor. *J Pediatr Surg* 2013; 48: 14-19.
- 6) KASTE SC, DOME JS, BABYN PS, GRAF NM, GRUNDY P, GODZINSKI J, LEVITT GA, JENKINSON H. Wilms tumour: prognostic factors, staging, therapy and late effects. *Pediatr Radiol* 2008; 38: 2-17.
- 7) LEWIS BP, BURGE CB, BARTEL DP. Conserved seed pairing, often flanked by adenosines, indicates that thousands of human genes are microRNA targets. *Cell* 2005; 120: 15-20.
- 8) CALIN GA, CROCE CM. MicroRNA signatures in human cancers. *Nat Rev Cancer* 2006; 6: 857-866.
- 9) ALVAREZ-GARCIA I, MISKA EA. MicroRNA functions in animal development and human disease. *Development* 2005; 132: 4653-4662.
- 10) ZHAO X, LU C, CHU W, ZHANG B, ZHEN Q, WANG R, ZHANG Y, LI Z, LV B, LI H, LIU J. MicroRNA-124 suppresses proliferation and glycolysis in non-small cell lung cancer cells by targeting AKT-GLUT1/HKII. *Tumour Biol* 2017; 39: 1393383449.
- 11) JIANG X, LI H. MiR-1180-5p regulates apoptosis of Wilms' tumor by targeting p73. *Onco Targets Ther* 2018; 11: 823-831.
- 12) CUI M, LIU W, ZHANG L, GUO F, LIU Y, CHEN F, LIU T, MA R, WU R. Over-Expression of miR-21 and lower PTEN levels in Wilms' tumor with aggressive behavior. *Tohoku J Exp Med* 2017; 242: 43-52.
- 13) WANG HF, ZHANG YY, ZHUANG HW, XU M. MicroRNA-613 attenuates the proliferation, migration and invasion of Wilms' tumor via targeting FRS2. *Eur Rev Med Pharmacol Sci* 2017; 21: 3360-3369.
- 14) CHEN J, WANG L, MATYUNINA LV, HILL CG, McDONALD JF. Overexpression of miR-429 induces mesenchymal-to-epithelial transition (MET) in metastatic ovarian cancer cells. *Gynecol Oncol* 2011; 121: 200-205.
- 15) YE ZB, MA G, ZHAO YH, XIAO Y, ZHAN Y, JING C, GAO K, LIU ZH, YU SJ. MiR-429 inhibits migration and invasion of breast cancer cells in vitro. *Int J Oncol* 2015; 46: 531-538.
- 16) LIU X, LIU Y, WU S, SHI X, LI L, ZHAO J, XU H. Tumor-suppressing effects of miR-429 on human osteosarcoma. *Cell Biochem Biophys* 2014; 70: 215-224.
- 17) WU CL, HO JY, CHOU SC, YU DS. MiR-429 reverses epithelial-mesenchymal transition by restoring E-cadherin expression in bladder cancer. *Oncotarget* 2016; 7: 26593-26603.
- 18) ZHANG M, DONG BB, LU M, ZHENG MJ, CHEN H, DING JZ, XU AM, XU YH. MiR-429 functions as a tumor suppressor by targeting FSCN1 in gastric cancer cells. *Onco Targets Ther* 2016; 9: 1123-1133.
- 19) TIAN X, WEI Z, WANG J, LIU P, QIN Y, ZHONG M. MicroRNA-429 inhibits the migration and invasion of colon cancer cells by targeting PAK6/cofilin signaling. *Oncol Rep* 2015; 34: 707-714.
- 20) HUANG XY, YAO JG, HUANG HD, WANG C, MA Y, XIA Q, LONG XD. MicroRNA-429 modulates hepatocellular carcinoma prognosis and tumorigenesis. *Gastroenterol Res Pract* 2013; 2013: 804128.
- 21) ZHANG E, LI W, YIN D, DE W, ZHU L, SUN S, HAN L. C-Myc-regulated long non-coding RNA H19 indicates a poor prognosis and affects cell proliferation in non-small-cell lung cancer. *Tumour Biol* 2016; 37: 4007-4015.
- 22) LI YJ, WEI ZM, MENG YX, JI XR. Beta-catenin up-regulates the expression of cyclinD1, c-myc and MMP-7 in human pancreatic cancer: relationships with carcinogenesis and metastasis. *World J Gastroenterol* 2005; 11: 2117-2123.